Using Formation Factor to Define the Durability of Ultra-High Performance Concrete

Robert Spragg[1], Igor De la Varga[1], Luca Montanari[1], Benjamin Graybeal[2]

[1]SES Group, McLean, VA

[2]Federal Highway Administration, McLean, VA

Abstract

Ultra-high performance concrete (UHPC) has gained an increasing usage for a wide-range of applications in transportation infrastructure. UHPC tends to exhibit good performance with respect to durability, but there is an interest in 1) being able to quantify the durability and 2) using a rapid measurement to qualify the durability of UHPC-class materials within performance-related specifications (PRS). This study proposes the use of the formation factor, a material property that describes the pore network (i.e., porosity and pore connectivity), and can be related to diffusion properties. While this approach has been applied to concrete pavement mixtures in a recently released pavement PRS, this study will focus on its applicability specifically to UHPC. The paper provides a background of the formation factor, details the test method that is currently in development, shares results from a range of commercially available UHPC materials, and details how thresholds for a PRS could be established based on UHPC classes and exposure categories.

Keywords: UHPC, Concrete Durability, Formation Factor, Resistivity, Diffusion

1. Introduction and Background

UHPC-class materials are increasingly gaining interest in the field of civil engineering due to the wide variety of unique applications in which they have been shown to perform quite well, including but not limited to: overlays [1,2], repair of existing in-service elements [3,4], connections [5–7], and full size elements [8]. This class of materials is defined as follows by Graybeal [9]:

> *"UHPC is a cementitious composite material composed of an optimized gradation of granular constituents, a water-to-cementitious materials ratio less than 0.25, and a high percentage of discontinuous internal fiber reinforcement. The mechanical properties of UHPC include compressive strength greater than 21.7 ksi (150 MPa) and sustained postcracking tensile strength greater than 0.72 ksi (5 MPa). UHPC has a discontinuous pore structure that reduces liquid ingress, significantly enhancing durability as compared to conventional and high-performance concretes."*

While materials of such a low water-to-cementitious materials ratio (w/cm) are quite durable if cracking is controlled, there has been an interest in 1) being able to succinctly quantify that durability and 2) identifying a rapid test method to qualify the durability of UHPC-class materials within performance-related specifications (PRS). Electrical measurements show great promise in this area and have been adopted for use in conventional concrete materials [10]. Electrical measurements in a medium with a single conductive phase, such as the pore fluid of the cementitious material, are a function of three parameters. Figure 1 illustrates these parameters with part (a) showing ρ_o which is the resistivity of the pore fluid, part (b) showing ϕ which is the volume of the pore fluid, and part (c) showing β which is the connectivity that describes how the pores are connected. It is often difficult to separate the influence of ϕ and β, so their inverse product is defined as the Formation Factor, shown in Equation (1) and often referred to as the F Factor [11].

ρ_o

ϕ

β

(a)   (b)   (c)
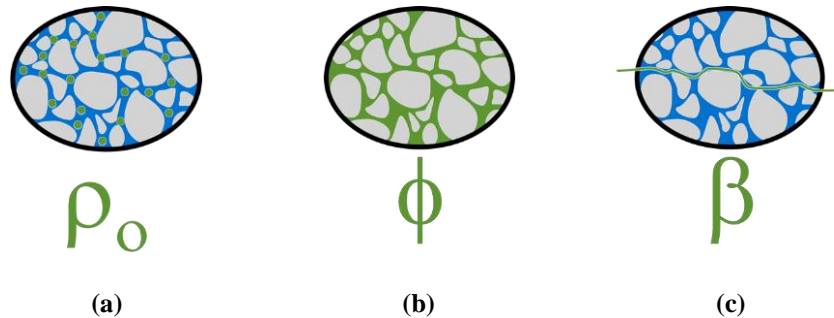
Figure 1. Parameters affecting electrical resistivity measurements in a single phase conductive medium.

$$F = \frac{1}{\phi\beta}$$

(1)

This study focuses on determining the F Factor through the use of a test method that allows for determination of key parameters. In this test method, three standard test cylinders are placed into a container with a solution of known composition. Rapid electrical measurements (which take less than 30 seconds) are periodically conducted on the cylinders. This study compares 4 commercially available UHPC materials with a typical 'non-shrink' cementitious grout and a

concrete similar in strength to a concrete used in precast elements. From the electrical measurements, the F Factor is determined for each material tested, and the results of the tests are contextualized using a diffusion based model.

2. Materials and Methods

2.1. *Materials and Conditioning*

The materials utilized in this study consisted of four commercially available UHPCs and are denoted as U1, U2, U3, and U4. The UHPC materials were typically supplied as: blended, premixed powder constituents; chemical admixtures; and steel fibers. The batch proportions were provided by the supplier, i.e., amount of water, admixtures, and fibers, along with mixing instructions.

The experiments in this study use electrical measurements to assess the microstructure of the materials, and the concepts used to derive the formation factor are only valid for a system where the single conductive phase is the pore fluid of the material. As such, the UHPCs were prepared without the steel fibers. While this would have a significant impact on the mechanical properties of the system, the authors believe it is necessary to accurately assess the microstructure using the rapid electrical methods in this study. Durability experiments assessing chloride transport by ponding, currently being conducted by the authors, indicate similar results for UHPCs with and without fibers, for a system that has not experienced cracking.

To provide a comparison to the values obtained from UHPC, two additional materials that are used in comparable applications were included in the testing program. The first one consisted of a concrete with 30% paste volume fraction, a w/cm of 0.35 by mass, and approximately 3% entrained air volume. The concrete was made with a Type I/II ordinary portland cement and local aggregates that met specifications for the Virginia Department of Transportation. The concrete mixture was designed to perform similarly to a precast concrete mixture and had a 28-d compressive strength of 7.5 ksi. In the study, the concrete is denoted as C. Additionally, a commercially available, 'non-shrink' cementitious grout was evaluated. It was mixed at a water to solids ratio of 0.16 as recommended by the manufacturer to obtain a flow of 100% according to ASTM C1437 [12]. The grout exhibited a 28-d compressive strength of 8.6 ksi and is denoted in the study as G.

The materials were mixed and placed into the cylinder molds and covered with the plastic lid. The group of specimens were covered with wet burlap and plastic sheet.At an age of 24 hours, the specimens were sealed in a heat-sealed 6-mil plastic bag. This is denoted as "sealed curing"; it prevents loss of moisture that might prematurely stop the hydration process, and also prevents excess moisture from entering the specimen to continue hydration. At the pre-established testing age, each specimen was removed from the plastic bag, demolded, and prepared for immediate testing. All testing and conditioning was conducted in a controlled environment of 23 +/- 2 °C (73 +/- 4 °F).

2.2. *Resistivity Testing*

The specimens in this study consisted of standard test cylinders, either 76 x 152 mm (3 x 6 inch) for the U materials or 102 x 203 mm (4 x 8 inch) for the G and C materials. At the desired testing age described below, the specimens were removed from the testing solution, surface dried using a towel, measured for their mass, and tested for resistivity using either surface resistivity (SR)

measurements, as described by AASHTO T358 [13], or uniaxial resistivity (UR) measurements, described by AASHTO TP119 [14]. The resistivity measurements are demonstrated in Figure 1.

(a)	**(b)**
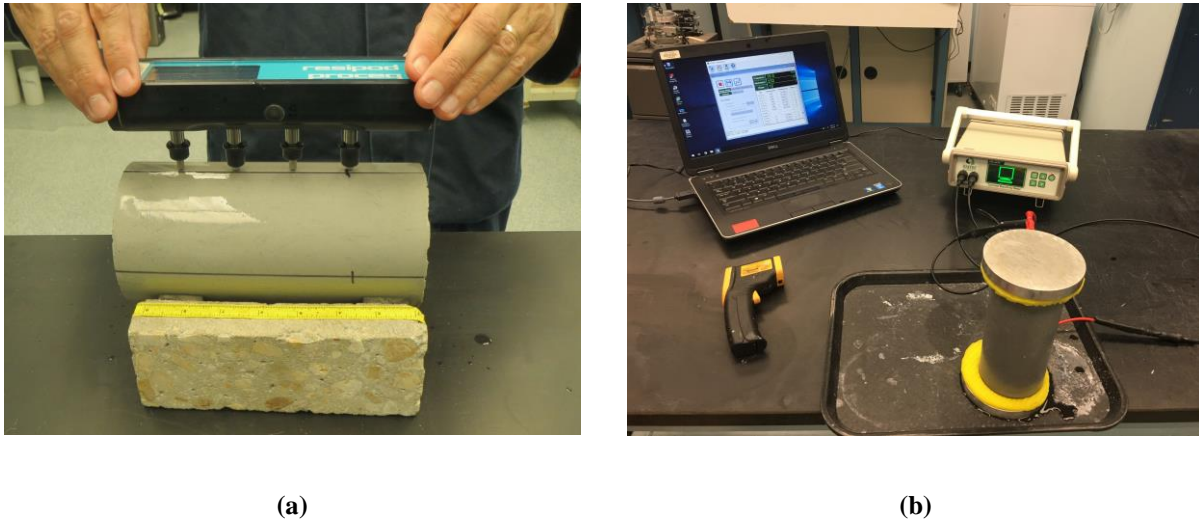
Figure 2. Resistivity measurements, using either (a) surface resistivity or (b) uniaxial resistivity.

The resistivity of the specimens (ρ) was calculated using a measured resistance value, R, and the geometry factor (k), as shown in Equation 2.

$$\rho = R \cdot k \tag{2}$$

The geometry factor, k, is dependent on the testing configuration. For the uniaxial configuration, k is the ratio of cross-sectional area to length, in units of meters. For the surface resistivity testing configuration, k is calculated as $2 \cdot \pi \cdot a / 2.69$, where a is the probe tip spacing in meters and 2.69 is a correction based on the specimen size [10,15]. Along with resistivity, the temperature of the specimens was recorded using an infrared thermometer. All temperature measurements were between 21 and 25 °C, so no additional corrections were needed to account for accelerated hydration or other effects on resistivity measurements [16].

2.3. Cylinder Absorption Test and Formation Factor Calculation

To determine the formation factor, a procedure termed the Cylinder Absorption Test (CAT) was from a similar method appearing in a recent guide specification for Performance Engineered Concrete Pavement Mixtures [17]. This similar method is currently a draft test method that has been submitted to the American Association of State Highway and Transportation Officials [18]. The method has been commonly referred to as the 'bucket test' as it can be conducted using a 5-gallon bucket [17,19–21]. After the specimens were sealed-cured for the specified curing period, the specimens were submerged into a storage solution of known composition and resistivity, detailed below. As the specimen absorbs the storage solution, the resistivity of the specimens is measured using the procedures defined above. Measurements were captured on each specimen for a period of about eight days after submersion in the solution, typically once every 24 to 48 hours. The G and C specimens were sealed-cured for 91 days prior to measurement capture. UHPC

specimens tend to express a resistance beyond the range of the instrumentation at 91 days, so the U series were sealed-cured for 7 days in one test series and 28 days in another.

The chemical composition of the solution mimics the pore solution composition of the cement-based material. The CAT test has been used extensively by researchers evaluating traditional concrete materials, and the recommended solution is a 0.5 M concentration solution of OH- (corresponding to a $\rho_s = 0.1\ \Omega \cdot m$) and is based on the estimated pore solution from a range of transportation related concrete mixtures [22]. The grout and concrete mixtures were evaluated with this solution (i.e., $\rho_s = 0.1\ \Omega \cdot m$). As UHPC has much lower w/cm and a high cement content, the estimated pore solution concentrations are much higher, based upon techniques described in literature [23–25], but can be confirmed in the future using experimental approaches [26]. As such, this study evaluated UHPC materials in the CAT using a solution of 1.16 M OH- concentration (corresponding to a $\rho_s = 0.05\ \Omega \cdot m$).

As the specimens absorb the storage solution, evidenced by the increase in mass of the specimens, the pores are filled in with the storage solution. That is to say, the storage solution becomes the specimen's pore solution. This is the major assumption of the CAT, namely that the properties of the storage solution are equivalent to the properties of the pore solution. There are many complexities that could arise from this assumption that are outside the scope of this paper, but the authors believe this is a good first step in approximating the pore solution properties, thus allowing for determination of the formation factor.

Following the above assumption, namely that the resistivity of the pore solution equals the resistivity of the storage solution ($\rho_o = \rho_s$), which was measured as $0.05\ \Omega \cdot m$ for the U specimens and $0.1\ \Omega \cdot m$ for the G and C specimens, the formation factor (F) can be determined at each testing age according to Equation 3:

$$F = \frac{\rho}{\rho_s}$$

(3)

3.   Results and Discussion

Once placed in the CAT solution, the cylinders gained mass as shown in Figure 3. The absorption in the C and G specimens was two to five times higher compared to the U specimens. A mass measurement is an important part of the testing program because it ensures that excessive moisture was not lost from the sample. Excessive moisture loss might artificially increase the F Factor measurement. It is recommended that a mass measurement be conducted at the same time as an electrical measurement, and that the mass measurement should not indicate a mass loss from the initial mass at the beginning of the test. For UHPC specimens the mass gain observed is expected to be in the range of 0.05% to 0.1%.
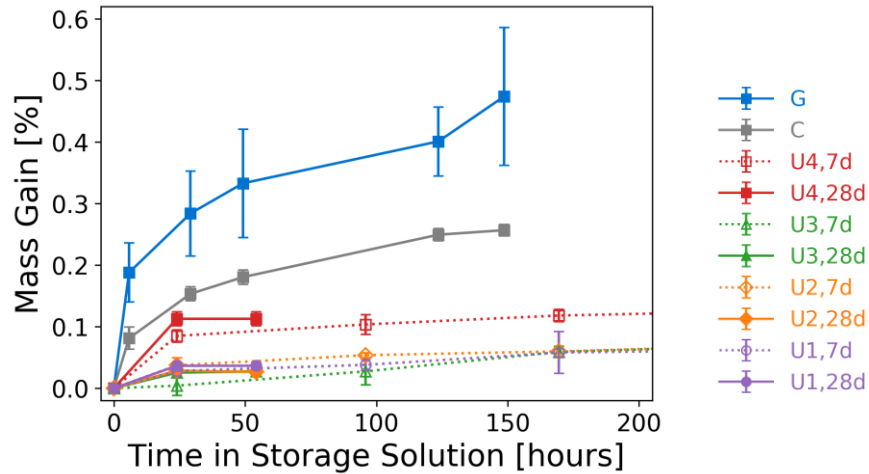
Figure 3. Mass change during the Cylinder Absorption Test indicates the pores filling in with the storage solution.

F Factor measurements during the bucket tests were conducted using two resistivity meters. Meter A was tested in both the Surface (SR) and Uniaxial (UR) configuration, while meter B was only tested in UR configuration. Comparing these measurements, shown in Figure 4, illustrates similar measurements for meter A and meter B, on average less than 4% different. Testing of UHPC typically exceeded the range of meter A, but the range meter B was not exceeded. Furthermore, the range of meter A in the SR configuration was slightly higher than the range in the UR configuration, which was in the range of 62,000 and 25,000, respectively. The difference in range is a function of testing geometry and specimen size and is not unexpected. This highlights that a test method for UHPC should have a consideration for when the material exceeds the upper-range of the equipment measurement capacity. This could be as simple as assuming if the measurement gives an off-scale error, that this maximum value be assumed. As a caution, it is also possible to obtain high F Factor values by excessive drying of the specimen prior to testing, even if only exposing the specimen to ambient lab conditions. This is the reason that care should be taken to minimize exposure time, and record mass as that would help to identify cases where a specimen might have been held out of solution prior to testing.
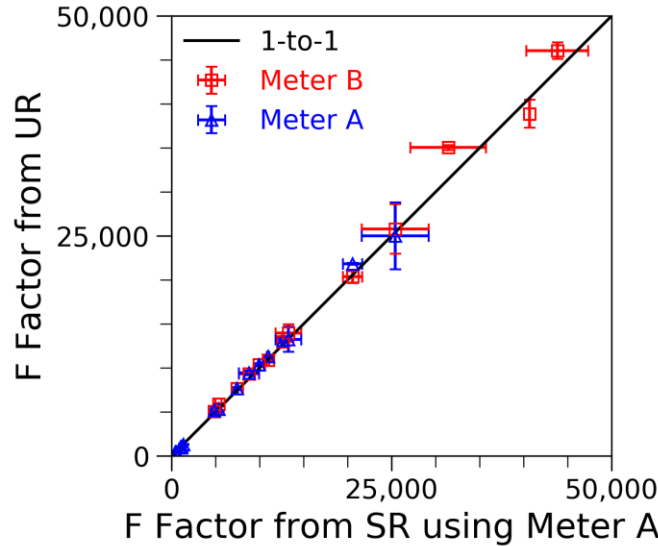
Figure 4. Comparison between F Factor measured using SR configuration with meter A to UR configuration of meter A and meter B.

Figure 5 illustrates that the F Factor of the U series were higher at both 7 and 28 days compared to the C and G specimens at 91 days. C and G specimens were not tested at earlier ages because their pore structure is still changing quite rapidly, and 91 day measurements were not obtained for U series due to the measurements outside the range of meter A, while meter B was added to the testing program too late for results to be included. The large range in F Factor values was observed for the U series, with values at 28 days ranging from 39,000 to 130,000. This wide range might have to either do with premixture development and particle packing effectiveness, the effective w/cm of the materials, or the chemistry of the cementitious materials. While outside the scope of this paper, F Factor values this high, while very different in terms of percentage, correspond to ion transport in extremely small pores. These small pore sizes, commonly referred to as gel pores, exist in the hydration products and are typically sized less than 10 nanometers ($3.94 \cdot 10^{-7}$ in).. As such, comparison between values this high should be considered carefully, as it does not necessarily mean that one UHPC performs three times better than another; instead, UHPC materials expressing responses in this range appear to all be exhibiting transport in the gel pore space. All the values from the U series, despite the large range, are much higher compared to traditional cement-based materials and will lead to a durable material, as discussed below.

To contextualize these values, the average F Factor values of the U Series at 7 day (7,820) and 28 day (79,400) are shown with dashed lines in Figure 5. As previously mentioned, there is a somewhat large range in the data, so a confidence interval, corresponding to +/- one standard deviation, is shown in the shaded region for each testing age (4,400 at 7 day and 44,100 at 28 day). As more data is obtained for this class of materials, the range of values will be helpful in establishing performance limits.
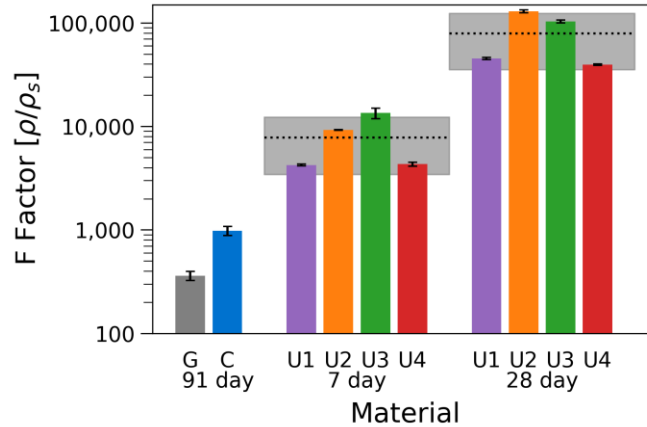
Figure 5. F Factor measurements obtained on Grout (G) and Concrete (C) at age of 91 d, and four different commercially available UHPCs (U1-U4) at 7 and 28 days.

The commercially available UHPCs evaluated in this study provided information for typical values of F Factor expected with UHPC class materials. To contextualize these results, a diffusion approach can be used to translate the F Factor into an engineering property. This approach uses the Error Function Solution to Fick's Second Law along with the Nernst-Einstein Equation to input F Factor (F) into the traditional Error Function solution, as shown in Equation 4:

$$\frac{C_{x,t} - C_o}{C_s - C_o} = 1 - erf\left(\frac{x}{2\sqrt{\frac{D_o}{F} \cdot t}}\right) \qquad (4)$$

where C_o is the background chloride concentration, typically assumed as 0.02%. $C_{x,t}$ is the chloride concentration at a depth x at a time t and is typically selected as 0.05%, which corresponds to the chloride concentration threshold typically associated with corrosion. D_o is the chloride ion self-diffusion coefficient, typically taken as a value of 19×10^{-10} m^2/s [27]. This particular example will use x as a 50-mm (2 in) cover depth and a surface concentration, C_s, of 0.5%, which is a moderate chloride exposure level [28]. More on this approach can found in literature [25].

Due to the large scatter in the F Factor values for the U series, a conservative approach is selected that uses the lower bound confidence interval that corresponds to the 28 day average minus one standard deviation, an F Factor value of 35,400. This value results in an estimated time to corrosion of 210 years. While this approach should not be interpreted as "UHPC will last 210 years", it does illustrate that a diffusion-based model for life-cycle estimation can be used to provide a sense of the UHPC-class materials response. In comparison, the G and C specimen results indicate an estimated corrosion initiation time of 2.2 and 5.7 years, respectively. As more UHPC-class materials are tested in upcoming studies, the values can serve to as a basis to establish performance limits in a performance-based specification for the durability of UHPC-class materials.
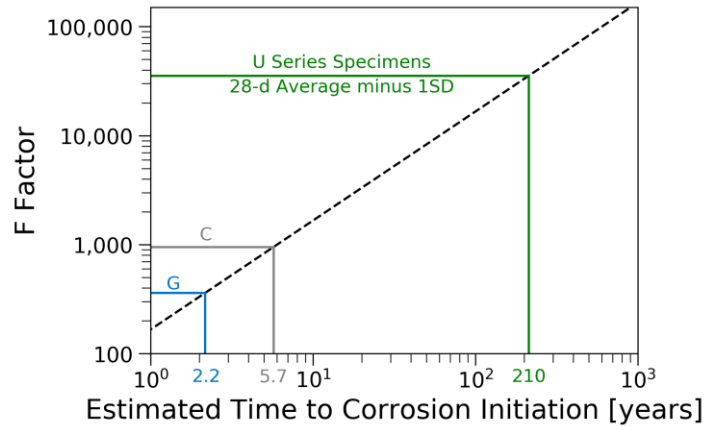
Figure 6. F Factor and estimated time to corrosion initiation at a moderate chloride surface concentration (0.5%) and a cover depth of 50 mm (2 in).

4. Conclusions

Formation Factor was presented and discussed as a tool to quantify the durability of porous materials. The Cylinder Absorption Test uses those concepts in a standardized way to assess formation factor for cement-based materials. The paper presented a very rapid testing methodology using two resistivity meters in two testing configurations where results differed by an average of less than 4%, meaning this method can be done with any AC resistivity meter. Each measurement takes less than 30 seconds, with one measurement conducted per day for 8 days. Mass measurements were conducted that showed UHPC specimens absorb much less solution than conventional materials; mass measurement should be included in a testing program to identify cases where excessive drying occurred that could lead to artificially high F Factor measurements. F Factor results from a wide range of commercially available UHPC-class of materials indicate results at 28 days that are significantly higher than traditional cement-based materials, which translates into much higher estimated times to corrosion initiation using Fick's Second Law. Based on the values at an age of 28 day, with a conservative assumption of the average minus one standard deviation of all four surveyed UHPCS, Fick's Second Law indicates an estimated time to corrosion initiation of 210 years. Future work will investigate additional UHPC-class materials, a further refinement of the storage solution, the influence of aging on F Factor values in UHPC-class materials, the role of chloride binding in UHPCs and on diffusion predictions, and an easily implementable F Factor procedure for quality assurance/quality control that could be used during construction.

5. References

[1] Haber, Z.B., Munoz, J.F., Graybeal, B.A., "Field Testing of an Ultra-High Performance Concrete Overlay," Federal Highway Administration, McLean, VA, Report No. FHWA-HRT-17-096, 2017.

[2] Haber, Z.B., Munoz, J.F., De la Varga, I., Graybeal, B.A., "Bond characterization of UHPC overlays for concrete bridge decks: Laboratory and field testing," *Construction and Building Materials*, Vol. 190, 2018. doi:10.1016/j.conbuildmat.2018.09.167.

[3] Nolan, S., "Prestressed/Precast Florida-Slab-Beams for Robust Local Bridges and

Accelerated Construction," Florida International University and the ABC UTC, Miami, Florida, 2017 Available at: https://abc-utc.fiu.edu/mc-events/prestressed-precast-florida-slab-beams-for-robust-local-bridges-and-accelerated-construction [Accessed: February 2, 2019].

[4]   Zmetra, K.M., McMullen, K.F., Zaghi, A.E., Wille, K., "Experimental Study of UHPC Repair for Corrosion-Damaged Steel Girder Ends," *Journal of Bridge Engineering*, Vol. 22, No. 8, 2017. doi:10.1061/(ASCE)BE.1943-5592.0001067.

[5]   Haber, Z.B., Graybeal, B.A., "Lap-Spliced Rebar Connections with UHPC Closures," *Journal of Bridge Engineering*, Vol. 23, No. 6, 2018. doi:10.1061/(ASCE)BE.1943-5592.0001239.

[6]   Graybeal, B.A., "Design and Construction of Field-Cast UHPC Connections," Federal Highway Administration, McLean, VA, Report No. FHWA-HRT-14-084, 2014.

[7]   Yuan, J., Zmetra, K.M., Graybeal, B.A., "Adjacent Box Beam Connections: Performance and Optimization," Federal Highway Administration, McLean, VA, Report No. FHWA-HRT-17-093, 2018.

[8]   El-Helou, R., Graybeal, B.A., "The Ultra Girder: A Design Concept for a 300-foot Single Span Prestressed Ultra High-Performance Concrete Bridge Girder," In: *Proceedings of the 2nd International Interactive Symposium on Ultra-High-Performance Concrete*, Albany, New York, 2019.

[9]   Graybeal, B.A., "Ultra-High Performance Concrete," Federal Highway Administration, McLean, VA, Report No. FHWA-HRT-11-038, 2011.

[10]   Spragg, R.P., Bu, Y., Snyder, K.A., Bentz, D.P., Weiss, J., "Electrical Testing of Cement-Based Materials: Role of Testing Techniques, Sample Conditioning, and Accelerated Curing," Joint Transportation Research Program, Indiana Department of Transportation, and Purdue University, West Lafayette, Indiana, Report No. FHWA/IN/JTRP-2013/28, 2013. doi:10.5703/1288284315230.

[11]   Rajabipour, F., "Insitu electrical sensing and material health monitoring in concrete structures," PhD, Purdue University, 2006.

[12]   ASTM C1437, "Standard Test Method for Flow of Hydraulic Cement Mortar," ASTM International, West Conshohocken, PA, 2015. doi:10.1520/C1437-15.

[13]   AASHTO T358, "Standard Method of Test for Surface Resistivity Indication of Concrete's Ability to Resist Chloride Ion Penetration," American Association of State Highway and Transportation Officials, Washington, D.C., 2015.

[14]   AASHTO TP119, "Standard Method of Test for Electrical Resistivity of a Concrete Cylinder Tested in a Uniaxial Resistance Test," American Association of State Highway and Transportation Officials, Washington, D.C., 2015.

[15]   Morris, W., Moreno, E.I., Sagüés, A.A., "Practical evaluation of resistivity of concrete in test cylinders using a Wenner array probe," *Cement and Concrete Research*, Vol. 26, No. 12, December 1996. doi:10.1016/S0008-8846(96)00175-5.

[16]   Spragg, R.P., Villani, C., Snyder, K.A., Bentz, D.P., Bullard, J.W., Weiss, W.J., "Factors That Influence Electrical Resistivity Measurements in Cementitious Systems,"

Transportation Research Record: Journal of the Transportation Research Board, Vol. 2342, December 2013. doi:10.3141/2342-11.

[17] AASHTO PP84, "Standard Practice for Developing Performance Engineered Concrete Pavement Mixtures," American Association of State Highway and Transportation Officials, Washington, D.C., 2018.

[18] Weiss, W.J., Tsui-Chang, M., Montanari, L., Qiao, C., Suraneni, P., "Develop and Deploy Performance-Related Specifications (PRS) for Pavement Construction," Federal Highway Administration and Oregon State University, McLean, VA, Report No. DTFH61-13-C-00025, 2017.

[19] Todak, H., "Durability Assessments of Concrete Using Electrical Properties and Acoustic Emissions," MSCE, Purdue University, 2015.

[20] De la Varga, I., Spragg, R.P., Muñoz, J.F., Helsel, M.A., Graybeal, B.A., "Cracking, bond, and durability performance of internally cured cementitious grouts for prefabricated bridge element connections," *Sustainability (Switzerland)*, Vol. 10, No. 11, 2018. doi:10.3390/su10113881.

[21] Akhavan, A., Rajabipour, F., "Evaluating ion diffusivity of cracked cement paste using electrical impedance spectroscopy," *Materials and Structures*, 2012. doi:10.1617/s11527-012-9927-x.

[22] Spragg, R.P., "Development of Concrete Performance Specifications that Include Formation Factor," PhD, Purdue University, 2017.

[23] Taylor, H.F.W., "Cement chemistry," Thomas Telford Ltd, London, 1997.

[24] Bentz, D.P., "A virtual rapid chloride permeability test," *Cement and Concrete Composites*, Vol. 29, No. 10, 2007. doi:10.1016/j.cemconcomp.2007.06.006.

[25] Spragg, R.P., Qiao, C., Barrett, T.J., Weiss, W.J., "Assessing a concrete's resistance to chloride ion ingress using the formation factor," In: Poursaee, A. (Ed.), *Corrosion of Steel in Concrete Structures*, Woodhead Publishing, London, 2016. doi:10.1016/B978-1-78242-381-2.00011-0.

[26] Tsui Chang, M., Montanari, L., Suraneni, P., Weiss, W.J., "Expression of Cementitious Pore Solution and the Analysis of Its Chemical Composition and Resistivity Using X-ray Fluorescence," *Journal of Visualized Experiments*, No. 139, 2018. doi:10.3791/58432.

[27] Haynes, W., ed., "CRC Handbook of Chemistry and Physics," CRC Press, Boca Raton, FL, 2010.

[28] Life-365, "Life-365 User Manual," Life 365 Consortium, 2012 Available at: http://www.life-365.org/.

6. Acknowledgements